

STRUCTURAL HEALTH MONITORING OF A WIND TURBINE WING USING NEURAL NETWORKS

PATERAKIS EMMANOUIL

10/07/2019

Abstract

Due to the stochastic nature of environmental loadings, a lot of interest is paid in the discovery of possible damages of the involved equipment in modern industry. In wind turbine's blades, where access is difficult and expensive, the development of a smart structural health monitoring system is essential. In the present paper, a large-scale composite wind turbine blade model is designed and used for the detection of several damage scenarios. The process which is presented here is mainly based on the development of monitoring techniques which exploit the capabilities of artificial neural networks. These techniques can provide the exact position of possible damages, under given external loading scenarios. Moreover, the use of such methods decreases significantly the need of external intervention and at the same time it increases the accuracy of the whole approach. The above processes are simulated using the finite element method.

Acknowledgment

For the about work, i would like to thank me supervisor,Prof. Stavroulakis Georgios and also his associate Koutsianitis Panagiotis, for all the help and guidelines they provided me. I would also like to thank them for the opportunity they presented to me by offering me to contribute to the creation of the paper. The research work was supported by the Hellenic Foundation for Research and Innovation (HFRI) and the General Secretariat for Research and Technology (GSRT), under the HFRI PhD Fellowship grant (GA. no. 34254).

Contents

1	Design of the airfoil -Principles	6
2	Materials and Manufacturing	7
3	Assumptions Definition	8
3.1	The location	8
3.2	Location Weather Conditions	8
3.3	Blade loads	9
3.4	Gravitational and Centrifugal Loads	10
3.5	Structural Load Analysis	10
4	Wind Turbine Blade	11
4.1	Orientation	11
4.2	Wind Turbine Blade	11
4.3	Blade Aerodynamics	12
4.4	Other Design Considerations	14
4.5	The Wind Turbine Blade Design	15
4.6	Blades 15 to 25 Meters in Length	15
5	Structural Health Monitoring	16
5.1	Structural Health Monitoring(SHM) and system in general	16
5.2	Assessment of Structural Health Monitoring Implementation	16
5.3	Drawbacks of Composite materials	17
5.4	Requirements of SHM for Composite materials	17
5.5	Damage identification and Structural Health Monitoring	18
6	Neural Networks	19
6.1	Artificial Neural Networks	19
6.2	Mathematical model of the neuron	19
6.3	Multi-layer perceptron	20
6.4	Back-propagation Network	21
6.5	Neural Network of the inverse problem	24
7	Numerical Results	25
7.1	Wind blade materials	25
7.2	Identification of cracks using neural networks	26
8	Conclusion	31
9	References	32

Introduction

Wind turbines are large rotating machines which have the ability to harvest and convert wind (kinetic) energy into mechanical power and subsequently to electricity through the use of a suitable generator. However, these large systems consist of several smaller parts, i.e. blades, joints, etc., which in turn are subjected to high wind or other loadings, as well as other environmental phenomena which could possibly put at risk the integrity of the whole structure. These residual forces can decrease significantly the lifetime of the critical components of wind turbine structures, such as the wind turbine blades, causing partial failures or even a total fail - sometimes catastrophic - of the whole system.

In the present investigation, a composite large-scale wind turbine blade model will be considered similar to the one presented in (Rentoumis et al., 2018). More specifically, a large-scale wind turbine blade of span which equals to approximately 25m, is taken in consideration. The location of installation is the Mount Panachaiko, Peloponnese, Greece. In order to assess the integrity of the blade structure, a damage identification algorithm based on neural networks is considered (Stavroulakis and Antes, 1998b).

The blade is hollow, which means that the outer geometry is formed by two separate shells; one on the suction side and one on the pressure side. The design of the airfoil considers both aerodynamic, as well as structural aspects. As for the aerodynamic considerations, they are vital for the design of the outer shell of the wind turbine blade, while structural aspects are considered for the design of the inner structure of the blade (Jensen, 2008).

The objective of the present paper is the development of a procedure for non-destructive crack identification in wind turbine blades. This methodology can be applied to damage identification, flaw detection, etc. Only static loads are considered here, while structural analysis is based on a finite element model with several failure scenarios. The inverse is solved by means of a back-propagation trained neural network. The training data are produced by the numerical model (pseudoexperiments).

Identification problems belong to inverse problems, due to the fact that even if some input-output data are available by measurements, the parameters values which are involved in the system remain unknown. In fact, the output error identification problem, which is the case here, is treated as an optimization problem for the difference between measurements and the desired values of parameters. The classical optimization approach is not always advantageous due to the nature of the problem. More specifically, for inverse problems, small variations of a certain structural parameter may lead to either large or small variations in the structural response depending on the position and/or the type of the parameter (Stavroulakis and Antes, 1998b). Due to this, the problem is considered to be an ill-posed one (Natke, 1991). Due to several nonlinearities, the arising optimization problem is usually nonconvex and thus, the possibility of multiple mathematical solutions exists. In terms of optimization, this corresponds to a problem with several local minima, and thus, the convergence of classical optimization algorithms is not always guaranteed. In this case, soft computing techniques, such as the neural network approach, which have the ability to overcome local minima, can be adopted.

The methodology used here for the treatment of the inverse problem has been developed and tested for the solution of crack identification problems in (Stavroulakis and Antes, 1998a). In previous publications, a two-dimensional specimen is considered which contains an un-

known crack. The unknown crack has been parametrized by a certain number of parameters, namely, the length of a linear crack, and the coordinates of the middle point with respect to the used global coordinate system. It is assumed that certain boundary displacements can be measured for various static, time-periodic or time-history external loading. The direct mechanical problem is solved numerically by the BEM method, while the identification (inverse) problem is treated by a neural network-based optimization technique. Details can be found in the papers (Jensen, 2008), (Stavroulakis and Antes, 1998a, 1999a, 1999b), (Stavroulakis et al. 2004). Recent investigations of our group present the defect identification of concrete piles by using dynamic test loading and neural networks, see (Protopapadakis et al., 2016) (Psychas et al., 2016).

1 Design of the airfoil -Principles

The design of the airfoil is the balanced output of two considerations that include: (i) the aerodynamic and (ii) the structural aspect of it. Aerodynamic considerations are the ones dictating the design of the outer shell of the blade while structural considerations are more vital for the design of the inner of the blade (Mølholt, 2008). Structurally, the blade is typically hollow, with the outer geometry formed by two separate shells: one on the suction and one on the pressure side. In order to transfer shear loads, one or more structural webs of different geometries are fitted to support and join the two shells together (see Figure 1).

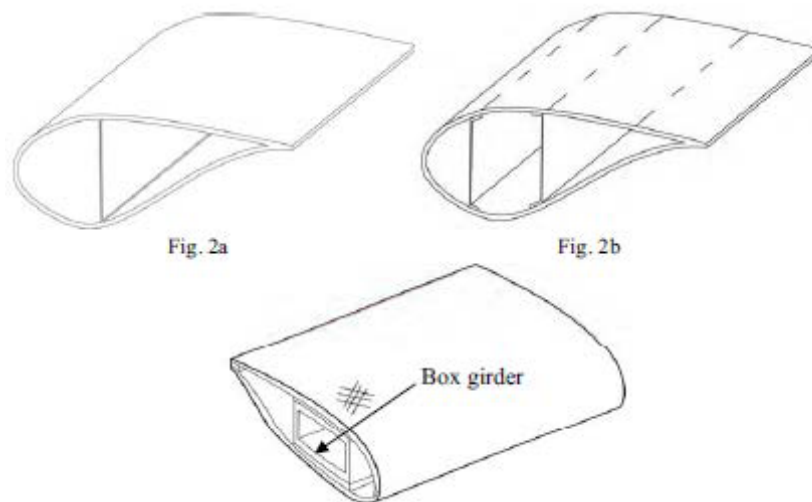


Figure 1: Sketches of various blade design approaches: (4a) Single shear web, (4b) Double shear web, (4c) With load carrying box girder. (Mølholt, 2008)

also Figure 3). In Figure 2, three different manufacturers' blade designs (LM Glasfiber, SSP Technology & Vestas) are presented. In the blade from LM Glasfiber (see also Figure 2a) an upper shell, a lower shell and two webs are bonded together to form the blade structure as shown in Figure 2b. In the blade from SSP-Technology a load carrying box girder is created

of two half parts bonded together while, in Figure 2c, Vestas uses a box girder which is manufactured on a mandrel.



Figure 2: Different wind turbine blade designs: (2a) LM-Glasfiber design, (2b) SSP-Technology design, and (2c) Vestas design. (Mølholt, 2008)

2 Materials and Manufacturing

Nowadays, there is a wide range of materials and manufacturing techniques utilized in the wind turbine industry. The most utilized material combinations used are composite laminates with embedded threaded steel rods in the root section, connecting the blade to the hub in a bolted connection. Polyester, vinyl ester and epoxy resins are common, matched with reinforcing wood, glass, and carbon fibers. A wide range of manufacturing processes are also utilized in blade manufacturing, encompassing: wet lay-up, pre-preg, filament winding, pultrusion, and vacuum infusion (with and without secondary adhesive bonding). More details can be found in ref. (US National Research Council) of 1991. In the first chapter of this report, the assumptions and restrictions taken into consideration will be presented including the location of the installation and the average weather conditions taking place according to officially published data. In the second chapter, the nominal loads to be applied will be defined, taking into consideration the industry's standards. In the third chapter, an introduction of the SHM methodology that will be carried out followed by the fourth chapter describing the material property requirements.

3 Assumptions Definition

3.1 The location

Mount Panachaiko is the most northern mountain of the Peloponnese state area and is occupying the north-central area of Achaia State. More accurately, it is situated eastern of the city of Patra. The highest peak of Mount Panachaiko has an altitude of 1925m. The largest Wind turbine farm of Greece is located in its north section, between the cities of Patra and Rio. The farm (ELEV: 1588 m LAT: 38deg 12min LONG: 21deg 54min) was established in 2006 and hosts 40 large scale wind turbines.

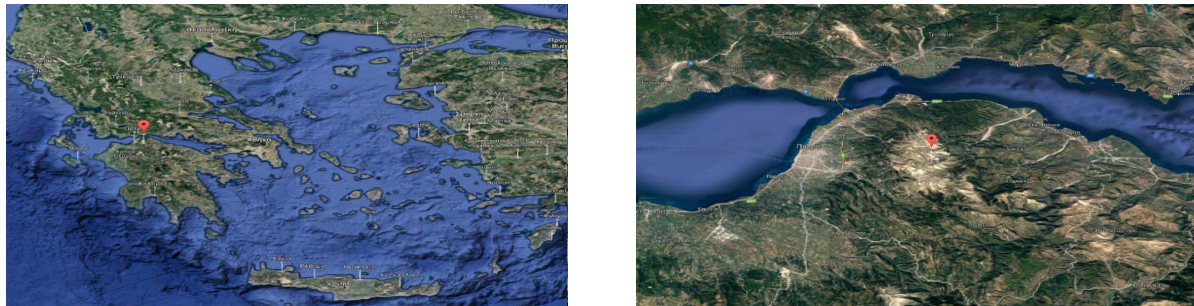


Figure 3: Panachaiko Mountain location in the northern area of Peloponnese, Greece. (Google Earth)

3.2 Location Weather Conditions

In order to have a better insight of the weather conditions that take place at Mount Panachaiko Mountain we accessed the National's Observatory of Athens Database.



Figure 4: View from Wind Farm of Mount Panachaiko. City of Patra at the left of the photo. (Google Earth)

3.3 Blade loads

The use of computer analysis software such as fluid dynamics (CFD) and finite element (FEA) is now commonplace within the wind turbine industry (Quarton, 1998). Dedicated commercially available software such as LOADS, YawDyn, MOSTAB, GH Bladed, SEACC and AERODYN are utilized to perform calculations based on blade geometry, tip speed and site conditions (Habali, 2000). To simplify calculations, it has been suggested that a worst case loading condition has to be identified compared to which all other loads may be tolerated (Gasch et al., 2002). The worst case loading scenario is dependent on blade size and method of control. For small turbines without blade pitching, a 50-year storm condition would be considered as in the limiting case. For larger turbines ($D \geq 70$ m), loads resulting from the mass of the blade become critical and they should be considered. In practice, several load cases are considered with published methods detailing mathematical analysis for each of the IEC load cases (Burton, 2011). For modern large scale turbine blades, the analysis of a single governing load case is not sufficient for certification. Therefore, multiple loading cases are analyzed. The most important load cases are dependent on individual designs. Typically priority is given to the following loading conditions:

- Emergency stop scenario (Ahlstrom, 2006)
- Extreme loading during operation (Burton, 2011)
- Parked 50-year storm conditions (Kong et al., 2005)

Under these operational scenarios, the main sources of blade loading are listed below:

- Aerodynamic

- Gravitational
- Centrifugal
- Gyroscopic
- Operational

The load magnitude will depend on the operational scenario under analysis. If the optimum rotor shape is maintained, then aerodynamic loads are unavoidable and vital to the function of the turbine, considered in greater detail. As turbines increase in size, the mass of the blade is said to increase proportionately at a cubic rate. The gravitational and centrifugal forces become critical due to blade mass and are also elaborated. Gyroscopic loads result from yawing during operation. They are system dependent and generally less intensive than gravitational loads. Operational loads are also system dependent, resulting from pitching, yawing, breaking and generator connection and can be intensive during emergency stop or grid loss scenarios. Gyroscopic and operational loads can be reduced by adjusting system parameters. Blades which can withstand aerodynamic, gravitational and centrifugal loads are generally capable of withstanding these reduced loads. Therefore, gyroscopic and operational loads are not considered within this work.

3.4 Gravitational and Centrifugal Loads

Gravitational centrifugal forces dependent to mass which is generally thought to increase cubically by increasing turbine diameter (Brondsted et al., 2006). Therefore, turbines under ten meters diameter have negligible inertial loads, which are marginal for 20m upwards, and critical for 70m rotors and above. The gravitational force is simply defined as mass multiplied by the gravitational constant, although its direction remains constant acting towards the center of the earth which causes an alternating cyclic load case. The centrifugal force is a product of rotational velocity squared and mass and always acts radial outward, hence the increased load demands higher tip speeds. Centrifugal and gravitational loads are superimposed to give a positively displaced alternating condition with a wavelength equal to one blade revolution.

3.5 Structural Load Analysis

Modern load analysis of a wind turbine blade would typically consists of a three dimensional CAD model analyzed using the Finite Element Method (Jensen, 2006). Certification bodies support this method and conclude that there is a range of commercial software available with accurate results (Veritas, 2010). These standards also allow the blade stress condition to be conservatively modeled using classical stress analysis methods. Traditionally, the blade would be modeled as a simple cantilever beam with equivalent point or uniformly distributed loads used to calculate the flap wise and edgewise bending moment. The direct stresses for root sections and bolt inserts would also be calculated.

4 Wind Turbine Blade

4.1 Orientation

There are two orientations of wind turbines: horizontal axis wind turbines (HAWT) and vertical axis wind turbines (VAWT). There are advantages and disadvantages to each orientation. VAWTs use drag forces to rotate their blades and are frequently referred to as drag machines. The dominant advantage to a VAWT is that it can accept wind from any direction at any time. This means that it does not require any yaw system to align the turbine in the direction of the incident wind field. The blades are commonly straight without any taper along the long axis. This allows them to be manufactured at lower cost. Since they rotate about the vertical axis the drive train can be located near the ground, which reduces the maintenance costs. Although VAWTs can accept wind from any direction, they are less efficient than HAWTs. Another major problem with VAWTs is their scalability in terms of viability for commercial production. They also tend to see larger fatigue damage on the blades at the rotor as a result of cyclic aerodynamic stresses (McGowan, 2000).

In contrast, HAWTs use lift forces to rotate their blades and are frequently referred to as lift machines. HAWTs can be designed such that the turbine is either upstream or downstream from the supporting tower. In the downstream version, the turbine automatically aligns its self with the wind; this rotation is known as yaw. To assist with their free yawing capability, the rotor blades are coned slightly in the downwind direction. Downstream HAWTs are influenced by tower wind shadow. Since the supporting tower is upstream of the rotor, a wake is created by the tower. The main effect of this wake is uneven air loading on the blades, which causes an uneven angle of attack on the blades and leads to decreased efficiency. In addition, the uneven cyclic loading causes fatigue damage not only to the blades but to the tower and drive train as well. To a lesser extent the downwind orientation also causes increased noise output.

In the upstream version, all tower wake effects are eliminated. However, the turbine is not capable of free yawing. This means that an active yaw control system is needed. These systems require a yawing motor, gears and a brake to hold the turbine in place when it is optimally oriented into the wind. Along with the increased complexity of a yaw control system, an increased torsional load is applied to the tower (McGowan, 2000).

A large advantage to HAWTs is the issue of solidity, which is defined as the ratio of the blade area to the swept blade area. As the turbine gets larger, the solidity gets smaller, which in-turn reduces the cost per kilowatt. HAWTs are also easier to mount on top of a large tower, which reduces the initial investment cost. As a result, HAWTs currently dominate the wind power market (McGowan, 2000).

4.2 Wind Turbine Blade

Energy is essential to human civilization development. With the progress of economics, there is an expanding demand on renewable energy resources to secure energy supply, like wind power, solar power, tide and wave power etc. As a clean renewable resource, wind power plays a more and more important role in modern life (RenewableUK 2012).

Power in the wind comes from the transformation of the air that is driven by the heat

of the sun, which is abundant, clean and renewable. As one of the most popular renewable energy resources, wind power exploitation is growing rapidly. At the beginning of 2006, the total installation of wind turbine capacity reached 59,206 MW worldwide (Schreck, S.J & Robinson, M.C. 2007). In June 2011, a total installation of 5,560 MW was operational and predicted by RenewableUK that in 2012 the annual wind power capacity will increase to 1.2 GW. It was also released by the Global Wind Energy Council that in 2011, a total annual increase in wind power industry reached 41 GW worldwide, which is corresponding to an annual growth of 21% comparing to the previous year. It has been estimated that the global capacity could reach no less than 200 GW by 2014. Wind turbine technology is undergoing great development. With the advancement of materials, manufacturing technology, intelligent control, and rotor aerodynamics, the rotor diameter of a 5 MW wind turbine (Re-power) has reached 126 meters (REpower 2012).

A wind turbine converts kinetic energy into mechanical power through a rotor, and then converts the mechanical power into electric power through a generator which is linked to the rotor with and without a gearbox. Various types of wind turbines are designed to take advantage of wind power based on the principles of aerodynamics. Depending on the wind turbine rotor orientation, there are two types of wind turbines, horizontal axis wind turbine (HAWT) and vertical axis wind turbine (VAWT). Based on the operation scheme, wind turbines can be divided into stall-regulated (fixed-pitch) wind turbines and pitch-controlled (variable-pitch) wind turbines. According to the relative flow direction of the wind turbine rotor, horizontal-axis wind turbines are either upwind or downwind turbines. Most modern HAWTs have three blades. Three-bladed upwind HAWT is the most common topology due to higher efficiency, better balanced performance and aesthetic appreciation. The fixed-pitch wind turbine remains one of the most popular topologies for wind turbines due to the advantages of simplicity, reliability, easy to access, well-proven and low cost. Most of wind turbines are three-bladed upwind fixed-pitch HAWTs, which are investigated in this thesis unless otherwise stated.

4.3 Blade Aerodynamics

A wind turbine is a complex system which consists of several components, including a rotor, a transmission system, a generator, a nacelle, a tower and other electro-mechanical subsystems. The rotor blades are the most important components. In order to transfer wind energy into mechanical and electric power, the blade is designed as an aerodynamic geometry with nonlinear chord and twist angle distributions. The section view of a wind turbine blade is of an airfoil shape (one or more airfoils), which is expected to generate high lift and low drag forces. The shape of the blade determines the energy captured, and the loads experienced. The study of interaction between wind flows and wind turbines is wind turbine aerodynamics which plays an important role in wind turbine design and analysis. Wind turbine aerodynamics comes from propeller aerodynamics. To introduce wind turbine aerodynamics in a simple way, a “tube” is introduced to describe the flow passing through a rotor in the classical disk theory.

In the disk theory, the flow is assumed equivalent across the sectional area of the tube, and the rotating rotor is regarded as a disc. When the inflow wind blows and strikes the blades, the velocity drops and the pressure increases just before the rotor plane and immediately

after the rotor plane, an adverse pressure distribution appears. With a pressure deficit between the upwind surface and the downwind surface along the span of the blade, once the total torque is able to conquer the cogging torque and the resistant torque of the system, the turbine rotor starts to rotate. With adequate wind inflow velocity (generally higher than 3-4 m/s), the turbine accelerates and the generator begins to produce electricity. An optimal wind turbine blade design usually has a high power efficiency, which is named as power co-efficient, and is calculated as the ratio of the rotor power output of the wind turbine to the power in the wind.

Many factors play a role in the design of a wind turbine rotor, including aerodynamics, generator characteristics, blade strength and rigidity etc. But wind energy conversion system is largely dependent on maximizing its energy extraction, rotor aerodynamics play important role in the minimization of the cost of energy. Moreover, there are many other aspects of concern in wind turbine blade design, such as maximum annual power capability, structure safety, economics, material availability and site suitability. All these factors contribute to CoE, which is the final goal of a wind turbine design. Wind turbine blade design is a multiple-objective optimization process as many disciplines are required including aerodynamic, structure, material, and economics. The design process is often executed in a heuristic manner.

The design process is composed of three main models which are a structure model, an aerodynamic model and an economics model (cost model). These three models form the main frame of wind turbine design. Among the three models, the aerodynamic model is the most fundamental one which determines the power extracted and the loads experienced. The structural design of blades is also as important as their aerodynamic design. The dynamic structural loads play the significant role in determining the lifetime of the rotor. In addition, the blade geometry parameters are required for dynamic load analysis of wind turbine rotors. As a result, the lifetime of wind turbine are all affected by the aerodynamic model used. In a word, the aerodynamic model has a great importance on design of wind turbine rotor blades and other components and subsystems. An aerodynamic model is the first consideration in the wind turbine design process.

4.4 Other Design Considerations

Several other design considerations include the categories of maintenance, environmental concerns, and wind resources. Maintenance can make up a significant portion of the overall cost of a wind turbine as maintenance costs tend to increase through the lifespan of the wind turbine. A benefit of increased turbine size is a decreased projected maintenance cost. Maintenance and capital cost can also be highly dependent on local labor and expertise.

Environmental concerns include noise pollution, aviation migration patterns, land use restrictions, local opposition, and electromagnetic interference (McGowan, 2000).

Wind resources need to be studied in depth before the implementation of any wind turbines. The higher the wind in the area, the more desirable the location; wind classes are based on power density and mean wind speed. Wind classes vary from class 1 to class 5, with class 1 being the least optimal for power production and class 5 being the most optimal. A wind class of at least 4 is required for a turbine to be reasonably productive (Elliott, et al., 1986). High wind environments also come with their issues. Because high wind may not always be constant, the variability of wind speeds may need to be studied. Higher wind areas also frequently have increased wind shear, gusts, and turbulence, all of which cause increased fatigue damage to wind turbines. Topography also plays a major role in wind patterns. This coupled with vegetation variations can cause greater surface roughness, requiring the supporting tower to be taller to get into the desired boundary layer level (McGowan, 2000).

4.5 The Wind Turbine Blade Design

Most of airfoil families are utilized for horizontal axis wind turbines (HAWTs) include among others NACA 44XX, NACA 23XXX, NACA 63XXX, and NASA LS series airfoils. All the above airfoils suffer noticeable performance degradation from roughness effects resulting from leading-edge contamination. The airfoil families are classified either as thick or thin. Thick airfoil families with thickness between 16% and 21%, are commonly found in stall-regulated wind turbines. Their utilization indicates that the tip-region airfoils are considered thick enough in order to accommodate overspeed-control aerodynamic devices and to reduce the blade weight. On the other hand, thin airfoil families those with thickness between 11% and 15%, are more suited to variable-pitch or variable-rpm turbines that use full-span blade pitch. In general, greater thickness is opted for the blade root airfoils to withstand structural and dynamic effects. The blade-root airfoil thickness is usually in the range of 18% to 24%. It has been assessed that thicknesses greater than 26% result to poor performance characteristics. In 1992, an airfoil family (Figure 5) was designed for extra-large blades for turbines rated at 400-1000 kW. This family, which is included in stall-regulated rotors, is composed of the S816, S817, and S818 airfoils. The tip-region airfoil has a $C_{l, \max}$ of 1.1 and a thickness of 16%. The primary outboard airfoil has a $C_{l, \max}$ of 1.2 and a thickness of 21% while the root airfoil has $C_{l, \max}$ of 1.3 and a thickness of 24% .

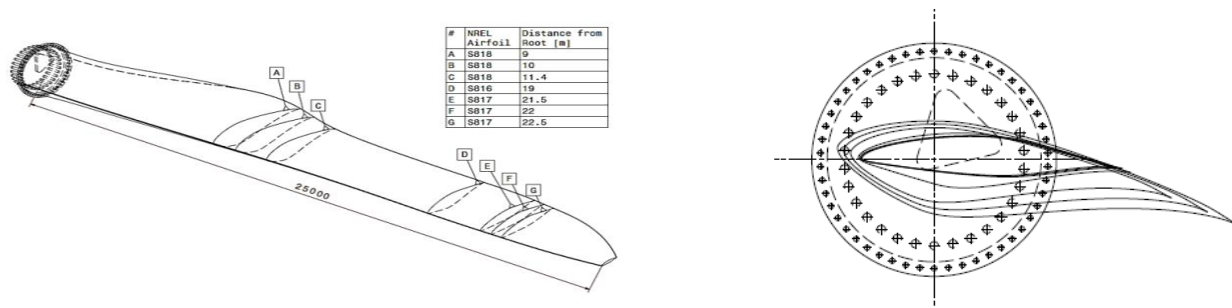
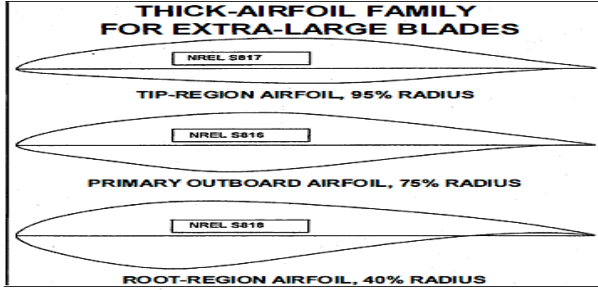


Figure 5: Illustration of airfoils location along the blade span and illustration of different pitch angles of airfoils with reference to the root of the blade.

4.6 Blades 15 to 25 Meters in Length

In 1992, an airfoil family (Figure 11) was designed for extra-large blades for turbines rated at 400-1000 kW. This family, which is included in stall-regulated rotors, is composed of the S816, S817, and S818 airfoils. The tip-region airfoil has a $C_{l, \max}$ of 1.1 and a thickness of 16%. The primary outboard airfoil has a $C_{l, \max}$ of 1.2 and a thickness of 21% while the root airfoil has $C_{l, \max}$ of 1.3 and a thickness of 24%.



Airfoil	r/R	Re. No ($\times 10^6$)	t/c	$C_{l, \max}$	$C_{d \max}$
S817	0.95	3.0	0.160	1.1	0.007
S816	0.75	4.0	0.210	1.2	0.008
S818	0.40	2.5	0.240	1.3	0.012

Figure 6: Thick Airfoil Family for extra-large blades (low tip C_l , max) and design specifications. (Somers, 1992)

5 Structural Health Monitoring

5.1 Structural Health Monitoring(SHM) and system in general

The first model of Structural Health Monitoring application began from aerospace industry during the 1970 and early 1980. Structural Health Monitoring and vibration-based damage have used, firstly, in the civil engineering community in the bridges and buildings. By the time, Structural Health Monitoring has expanded throughout the engineering. (Farrar and Worden, 2007)

In general, a Structural Health Monitoring system can be considered to be combined of two key factors, sensing technology and the associated signal analysis and interpretation algorithm. The data of Structural Health Monitoring consists of the response of the structure at different locations and information about the environmental conditions. Temperature, barometric pressure and wind speed are measurements related to the environmental conditions. Moreover, this system contains sensors which consists of three basic steps i.e., the signal monitoring, the processing and the interpretation. This systems are vibration-based, which are essential to avoiding problems and preventing of internal damages.

The collection of extract data, that systems have, can be useful information about the structure and its performance. This extract information can be used for decision-making regarding the safety, reliability maintenance, operation and future performance of the structure.

5.2 Assessment of Structural Health Monitoring Implementation

Structural failures are caused by several reasons, e.g. earthquakes, hurricanes, strong winds, extremely high temperatures etc. For that reason, a suitably defined system, able to monitor the performance of the whole structure, is necessary. For the case of wind turbines, this need is ubiquitous due to inaccessibility reasons (e.g. offshore structures), fatigue, or even because of the type of loads. A Structural Health Monitoring (SHM) system is a damage identification procedure for the prediction of possible damages of the host structure. Moreover, this system can take measures where necessary, which is very important as significant economic loss can be prevented. The whole procedure consists of three basic steps, i.e the signal monitoring, the processing, and the interpretation. Moreover, such systems

are vibration-based, thus vibrations can be used for the detection of internal damages which usually are hidden, and they cannot be observed (Bouزيد, 2015).

The core idea behind vibration-based SHM is that failures usually affect the dynamic characteristics such as for example the stiffness. This means that the severity of the damage can be quantified by its eigen-characteristics. To this extent, SHM is used for the detection of common failure scenarios (Ghoshal et al., 2000).

Composite materials which are used in wind turbines' blades have certain advantages, i.e. they improve the electrical conductance. However, they exhibit anisotropic properties which makes the mechanism behind failures sophisticated. This type of materials is usually suffering by ageing and fatigue. Moreover, even a small impact can lead to the creation of cracks, delamination phenomena on the fibers, etc. in-situ sensors with intelligent algorithms for on-line damage detection can be combined in order to achieve high accuracy and reliability for damage identification and monitoring at the minimum cost (Li et al., 2014).

5.3 Drawbacks of Composite materials

The wind turbines' blades are manufactured using composite materials which generally improve the electrical conductance and/or the energy harvesting efficiency. However, composites exhibit anisotropic properties which makes the mechanism behind the potential damages and failures quite complicated. Moreover, the absence of available standards holds back the design process and usually leads to overdesigned structures. Another, let say, drawback of composite materials is their sensitivity to damages due to impact loadings which is caused by the shortage of extra reinforcement. Cracks, delamination of fibers and/or other failures can be caused even by a minor impact. Finally, composites are influenced by ageing and/or material fatigue.

5.4 Requirements of SHM for Composite materials

Non-Destructive Testing (NDT) methods can be used for damage detection. However, these methods have some disadvantages as they require heavy equipment, they are time consuming (especially for large-scale structures such as wind turbines) and expensive, as they increase the maintenance cost. Structural health monitoring combines in-situ sensors with intelligent algorithms for on-line damage detection. This method can achieve high accuracy and reliability for damage detection at the minimum cost.

5.5 Damage identification and Structural Health Monitoring

In general, modal analysis tools can be very useful for damage identification as the dynamic characteristics of a smart structure are modified due to the existence of damages or failures. However, the case here is the identification of structural failures by using machine learning techniques such as neural networks. This means that the first step for damage identification can be either the conduction of a complete modal analysis or the consideration of a suitably defined and trained artificial neural network. In the present investigation, the cracks occur near the trailing edge of the blade structure close to the free end (see Figure 7).

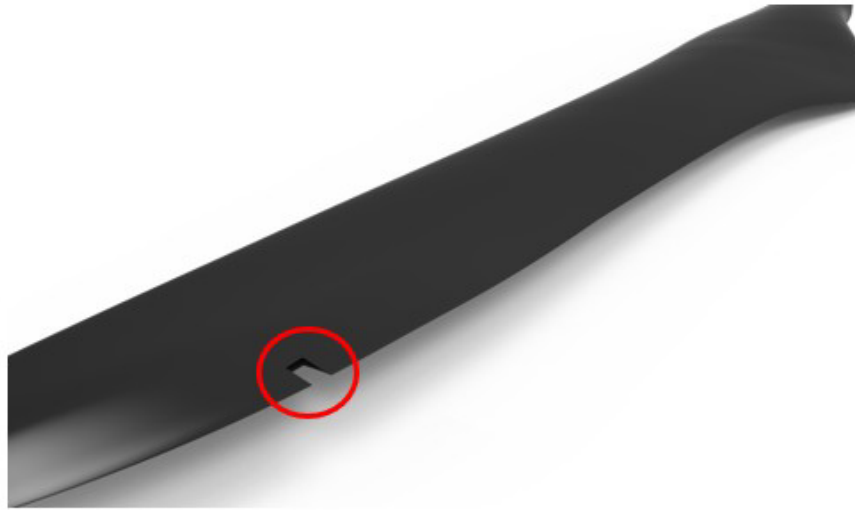


Figure 7: Positions of measurements (control points)

6 Neural Networks

6.1 Artificial Neural Networks

The Artificial Neural Networks is a machine learning prediction algorithm which attempts to simulate the function of the human central nervous system. Artificial Neural Networks is not considered as a complex algorithm for hardware implementation.(Kakoulli, E.,2012) First, it is about a network of interconnected calculating nodes (artificial neurons) which are algorithms of computational intelligence. A number of dimensional inputs are inserted throughout the Artificial Neural Networks which are initially multiplied by its initial weights. Then, if the weighted sum of the n dimensions exceeds a threshold value, then the neuron fires a floating point value which is the passed through the activation function for mapping the value to give an output. Even though the cost function is high , back-propagation algorithm achieve to have a low cost because of changing the weights of the Artificial Neural Networks. On every new iteration the weights are updated, so it can reach the lowest cost. Such multiple neurons together is known as a Neural Network. The basic operation of processing the inputs to predict the output, make the Artificial Neural Network design.

6.2 Mathematical model of the neuron

Biological neural networks are very complex. In contrast, the mathematical model of the network is much more simplified and is based on several assumptions:

1. All neurons are synchronized. That means that the signal passing from one neuron to another takes the same time for all connections. Signal processing is also synchronized and is the same for all neurons.
2. Every neuron has a so-called transfer function which determines neuron's output signal depending on the input signal strength. That function is time-independent.
3. When the signal passes the synapse, it changes linearly, i.e., the signal value is multiplied by some number. That number is called synaptic weight.

The very important property of the synaptic weight is that it changes in time. That feature makes it possible for brain to react differently on the same input in different moments. Or, in other words, to learn. Of course, those assumptions simplify the initial biological neural network very much.

For example, brain signal transmission time naturally depends on the distance between neurons. Artificial networks still preserve the most important characteristics of biological networks - adaptability and ability to learn.

The first mathematical model of the neuron was introduced more than a half century ago, but did not change much since then. First of all, the neuron is seen as a simple "automate" that transforms input signals into the output signal (Figure 8).

The model functions as follows: inputs of the neuron's synapses receive N signals $[X_1, \dots, X_n]$. Then every synapse makes a linear modi

fication of the signal using its synaptic weight. After that neuron's body (soma) receives signals $[X_1w_1, \dots, X_nw_n]$ (where w_i is the corresponding synaptic weight) and sums those

signals:

$$S = \sum_{i=1}^n X_i w_i$$

Then it applies some given function F (that is also called activation function) and sends the final signal:

$$Y = F(S)$$

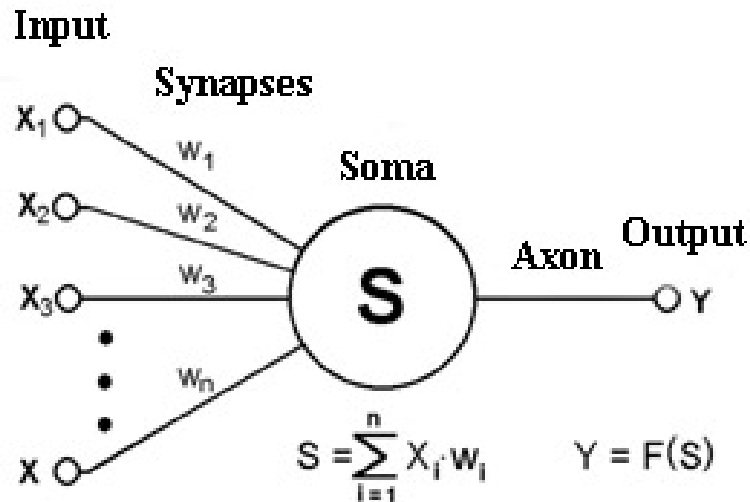


Figure 8: Artificial neuron model.

to the output. There are different functions, that are commonly used as activation functions. In a network, it is not necessary to use the same function for all the neurons. However, it's a common practice. In most cases activation functions are non-linear. Otherwise, the whole network will implement some linear transformation and will be equivalent to only one artificial neuron perceptron.

6.3 Multi-layer perceptron

That section describes one of the fundamental neural networks' types - multi-layer perceptron (or MLP, or back propagation network). Lots of other neural networks' types - such as RBF networks or probabilistic networks - are based on that model. In general, an artificial neural network is a set of artificial neurons. Arrangement and types of those neurons depend on the network type. Multi-layer perceptron contains three types of neurons:

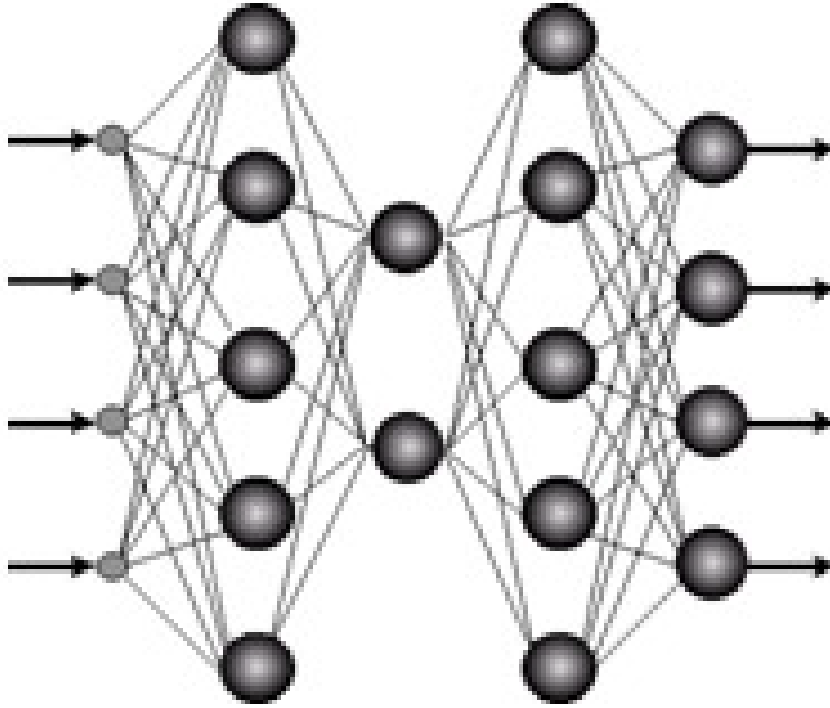


Figure 9: Multi-layer perceptron.

1. Input neurons. Those neurons are taking input vector that encodes some action or information about the external environment. Input neurons don't perform any type of computation, but only pass the input vector to subsequent neurons.
2. Output neurons receive signals from the preceding neurons and transform it using formulas. Those values represent output of the whole neural network.
3. Hidden neurons are the basis of the neural network. Those neurons receive the signal from the input neurons or preceding hidden neurons, process it in accordance with formulas and then pass result signals to the subsequent (hidden or output) neurons.

In multi-layer perceptron neurons are divided into layers. Input and output neurons form separate layer each - input layer and output layer. Hidden neurons form one or several hidden layers. Every MLP neuron, with the exception of input neurons, is connected via synapses with all neurons of the previous layer. Example of the MLP architecture is shown on Figure 9

6.4 Back-propagation Network

Neural Networks can be used for several applications, such as, solving different problems, damage identification(Natke, 1001), (Efstathiades et al., 2007),for optimization of control parameters (Muradova et al., 2016) etc. In order to do this, the network should be set up and trained.

First, the network selects, how many input and output neurons should contain and how many hidden neurons and layers. However, the selection of hidden units and layers is not

simple. Too few of them and you get high training error and underfitting, too many of them and get overfitting. (Lawrence S., 1997)

There are several ways of training a network. Back-propagation algorithm can be classified into supervised and unsupervised learning. Supervised learning is the process that combines the inputs that the network should learn which all together are the training set. Unsupervised learning means that the training set does not contain expected outputs for the given inputs.

This back-propagation method of errors training method calculates the derivative of the errors considering network weight. The derivative is fed to the optimization method which updates the weights and looks for the minimum value of the error function.

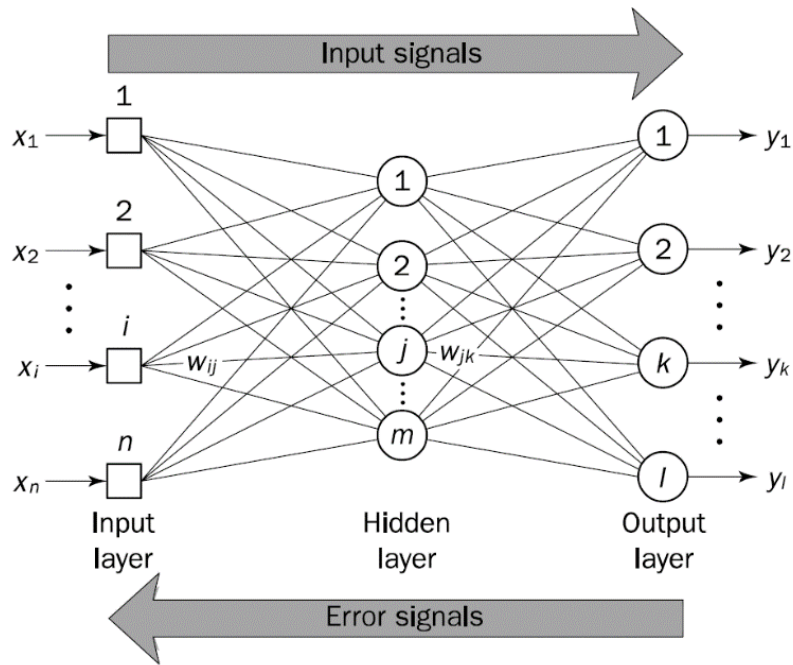


Figure 10: The backpropagation training process

A selected set of training data connects the measurements directly with failure characteristics. If there is an error in calculated outputs, the weights are adjusted to minimize the error. With this method, the neural network solves directly the inverse problem. In this case, this methodology can be used for static loading and measurements of displacements or deformations, for harmonic dynamic loading, for eigenvalues and eigenmodes or even for dynamic service loads or testing loading such as ultrasounds which are used in nondestructive structural evaluation.

6.5 Neural Network of the inverse problem

In the present investigation, a blade structure with an unknown crack is analyzed. The crack is characterized by a set of parameters $z = [z_1, \dots, z_m]^T$. Here, the coordinates (x, y) of the crack are used as identification parameters. The deformation of the blade for a given static loading $b^l, l = 1, \dots, l_1$ (see Figure 11) and for a given crack z is given by the vector $\tilde{x}(z, b^l)$.

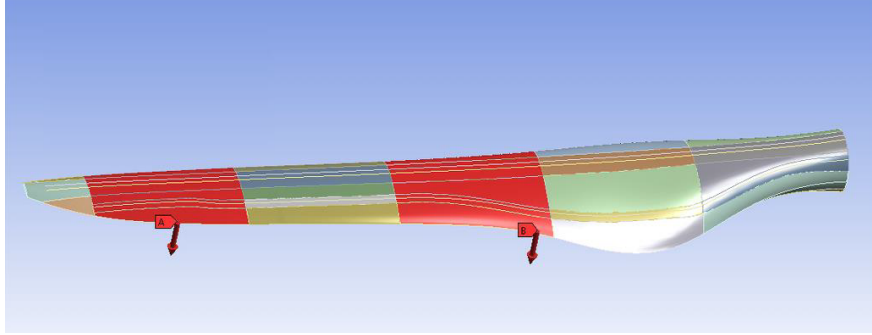


Figure 11: Areas of static loadings on the wind turbine blade

In this case, l_1 , is the total number of different loading cases. Moreover, let the response of the examined structure with a known crack be subjected to the same loading b_l denoted by $\tilde{x}_0(z, b^l)$. In this investigation the elements of $\tilde{x}_0(z, b^l)$ are produced by a finite element algorithm. The same procedure can be also used for the solution of the inverse analysis problem if a set of training data is available. Here, a direct solution of the inverse problem by means of back propagation trained neural networks is sought. Due to the appearance of nonlinearity in the response vector in terms of the crack parameters, the classical error minimization approach may lead to nonconvex optimization (Stavroulakis, 2013) (Stavroulakis and Antes, 1997). A multilayer back-propagation error trained neural network is used to learn the relation:

$$\tilde{x}(z, b^l) \rightarrow z$$

for a given value of loading vector b_l . The couples of data composed of the vectors $\tilde{x}(z, b^l)$ and the corresponding parameter vectors z are used as training examples. In the production mode, the nonlinear network reproduces the relation $x \rightarrow z$, i.e. for a given set of measurements \tilde{x} (different from the ones used in training) it gives a prediction for the variables characterising the internal crack (Stavroulakis and Antes, 1998b).

7 Numerical Results

7.1 Wind blade materials

The total structure is of sandwich form for both the external surfaces and the internal spars. The thickness of the structure differs from point to point. More material is necessary at the spars, where larger stiffness is needed, while the external surfaces are thinner, thus less material is used. Namely, the thickness at the different surfaces vary from 0,035 m to 0,1 m. The model which is considered in the present investigation consists of an isotropic elastic PVC foam, which is used for the core of the blade, while the external material is chosen to be an orthotropic elastic Epoxy Carbon material with enhanced characteristics in terms of electrical conductance, i.e. in terms of sensing ability, which is very useful in similar applications. The total mass of the blade is 3.686,39 kg. The characteristics and critical values of the materials which were used, are given in detail below. The detailed material properties of the foam are given in Table 1, while the ones for the Epoxy Carbon material are presented in Table 2.

Table 1: PVC foam material properties.

Density [kg/m ³]	80
Young's Modulus [Pa]	1,02x10 ⁸
Poisson's Ratio	0,3
Bulk Modulus [Pa]	8,5x10 ⁷
Shear Modulus [Pa]	3,9231x10 ⁷

Table 2: Epoxy Carbon UD material properties.

Density [kg/m ³]	1490
Young's Modulus (X direction) [Pa]	1,21x10 ¹¹
Young's Modulus (Y direction) [Pa]	8,6x10 ⁹
Young's Modulus (Z direction) [Pa]	8,6x10 ⁹
Poisson's Ratio (XY)	0,27
Poisson's Ratio (YZ)	0,4
Poisson's Ratio (XZ)	0,27
Shear Modulus (XY) [Pa]	4,7x10 ⁹
Shear Modulus (YZ) [Pa]	3,1x10 ⁹
Shear Modulus (XZ) [Pa]	4,7x10 ⁹

The orthotropic strain limits and the orthotropic stress limits of the Epoxy Carbon material are given in the following Table 3.

Table 3: Epoxy Carbon UD Orthotropic Strain and Stress Limits.

	Strain [m]	Stress [Pa]
Tensile (X direction)	$1,67 \times 10^{-2}$	$2,231 \times 10^9$
Tensile (Y direction)	$3,2 \times 10^{-3}$	$2,9 \times 10^7$
Tensile (Z direction)	$3,2 \times 10^{-3}$	$2,9 \times 10^7$
Compressive (X direction)	$-1,08 \times 10^{-2}$	$-1,082 \times 10^8$
Compressive (Y direction)	$-1,92 \times 10^{-2}$	$-1,0 \times 10^8$
Compressive (Z direction)	$-1,92 \times 10^{-2}$	$-1,0 \times 10^8$
Shear (XY)	$1,2 \times 10^{-2}$	6×10^7
Shear (YZ)	$1,1 \times 10^{-2}$	$3,2 \times 10^7$
Shear (XZ)	$1,2 \times 10^{-2}$	6×10^7

7.2 Identification of cracks using neural networks

In the present investigation two different cases are examined. The failures (cracks) appear on the surface of the wind turbine blade.

Case 1:

For the first numerical experiment, the control points (points of measurement) on the blade are selected on the central axis of the surface as shown in Figure 12. More specifically, 44 control points are employed for the analysis. A static analysis is performed on the wind turbine in order to obtain the training data for the neural network which is trained using the back-propagation method. A total amount of 40 cracks are used for the training process. Namely, the displacements for each crack are measured at these points in order to train the neural network for the detection of cracks. The same points of measurement are also used for the testing process. The results of the analysis are displayed below.

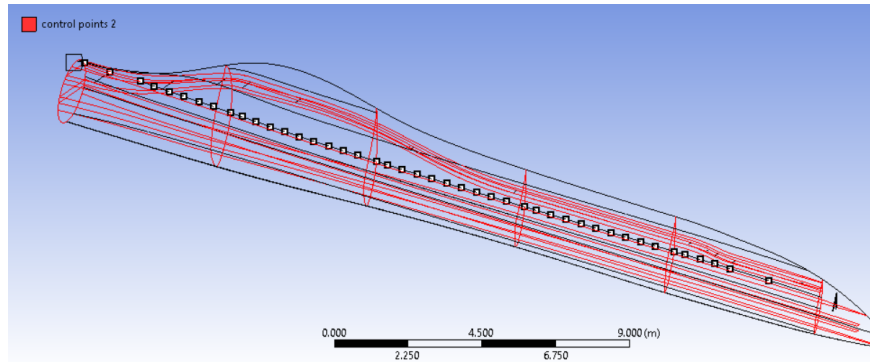


Figure 12: Positions of measurements (control points)

The results from the neural network are presented in Figure 13. With green circles are denoted the real position of the cracks, while with blue crosses are presented the predictions of the neural network. From these results, it is clear that the trained network can predict the positions of the recurring cracks very effectively.

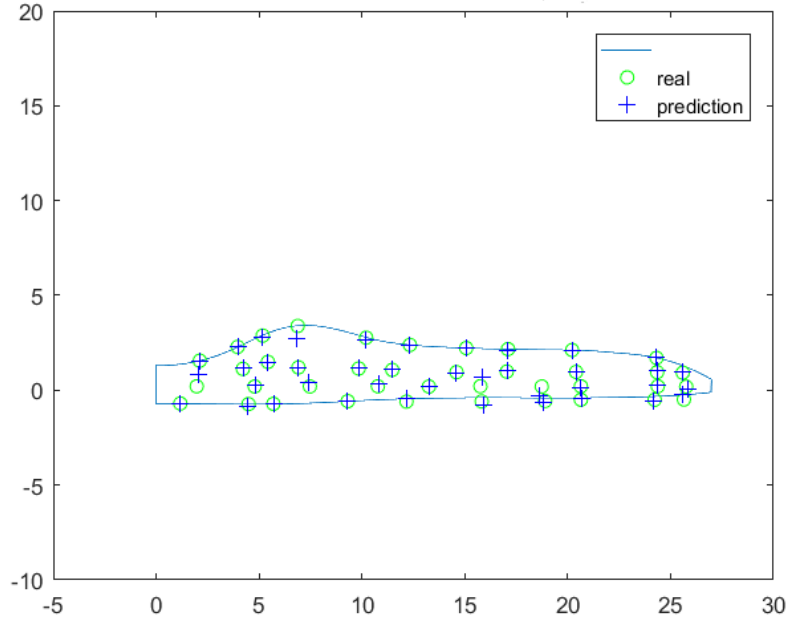


Figure 13: The results from training by the neural network

In Figure 14 one can see the correlation of inputs and outputs for both the model and the neural network prediction, as well as the error of the created system through the deviation of the diagonal line, which represents the error-free cases. Every point corresponds to a different damage example used for training or representation of the neural network model.

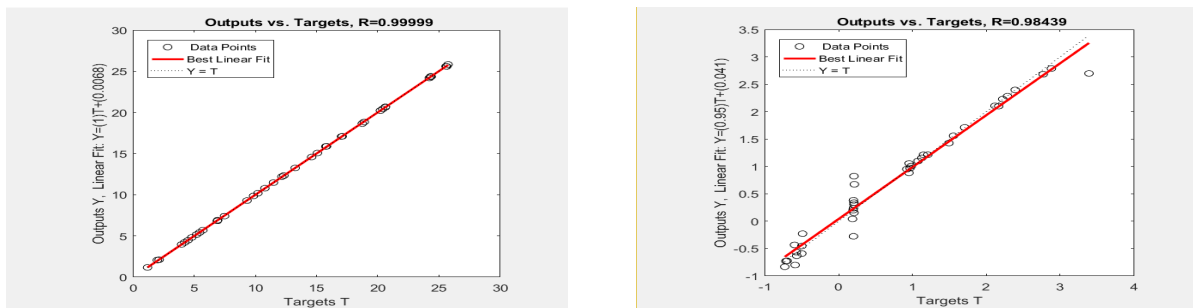


Figure 14: Correlation of inputs and outputs for both the model and the neural network prediction

A simulation with the use of 10 unknown cracks is performed. The results are shown in Figure 15. Again, with green circles are denoted the real position of the cracks, while with blue crosses are presented the predictions of the neural network.

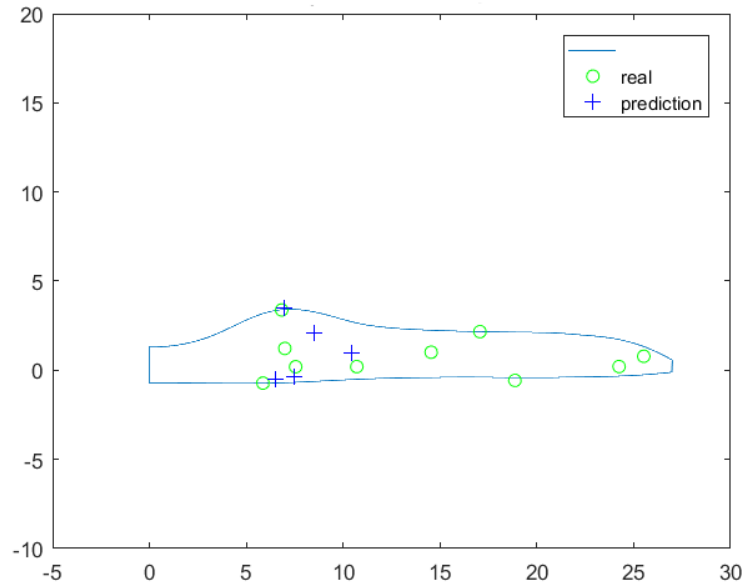


Figure 15: The results for the first case

In Figure 16 one can see the correlation of inputs and outputs for both the model and the neural network prediction, for case 1. From the results it is clear that the fitting is not sufficient.

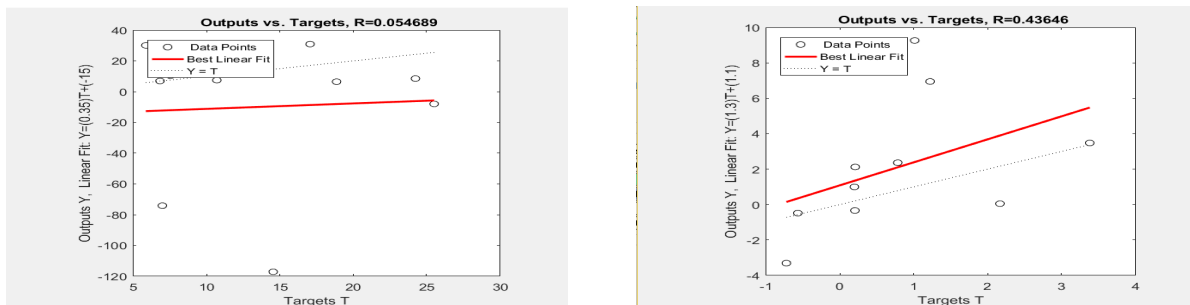


Figure 16: Correlation of inputs and outputs for both the model and the neural network prediction for case 1

Case 2:

For the second case, a set of 105 control points is selected, covering not only the central axis of the surface as in case 1, but the whole surface of the wind turbine blade, as seen in Figure 17. The same analysis is performed in order to obtain the training data for the neural network. A total amount of 40 cracks are used for the training process. Namely, the displacements for each crack are measured at these points in order to train the neural network for the detection of cracks. The same points of measurement are also used for the testing process. The results of the analysis are displayed below.

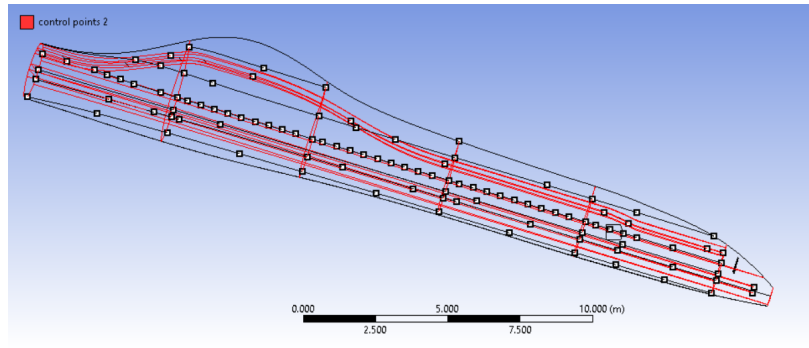


Figure 17: Positions of measurements (control points)

The results from the neural network are presented in Figure 18. Again, with green circles are given the real position of the cracks, while the blue crosses denote the predictions of the artificial neural network. It is seen that the trained network can predict even more efficiently the positions of the recurring cracks.

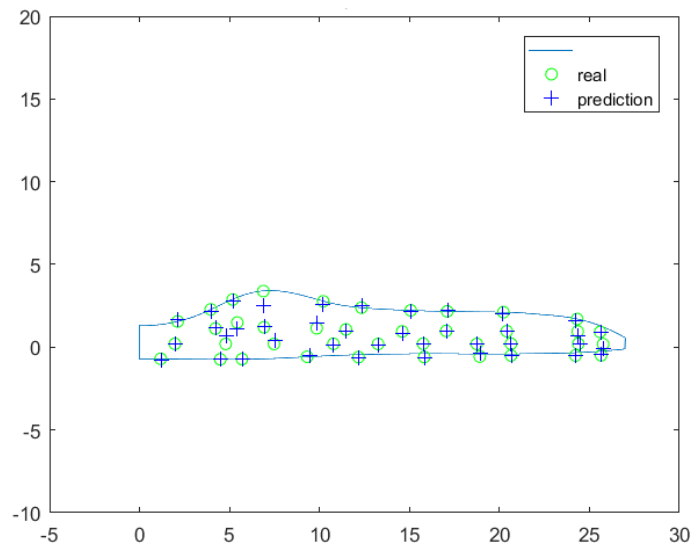


Figure 18: The results for the first case

In Figure 19 can see the correlation of inputs and outputs for both the model and the neural network prediction, as well as the error of the created system through the deviation of the diagonal line, which represents the error-free cases. Every point corresponds to a different damage example used for training or representation of the neural network model.

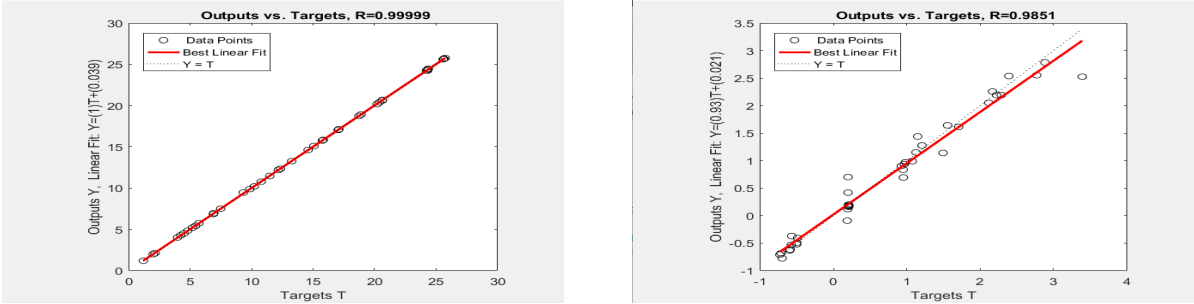


Figure 19: Correlation of inputs and outputs for both the model and the neural network prediction

The same 10 cracks are used for the analysis and the results are shown in Figure 20. The results here indicate that the training of the network in this second case is more successful.

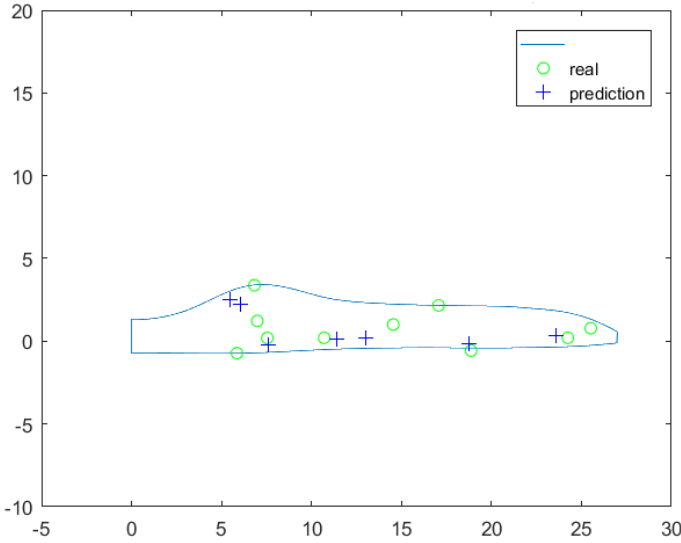


Figure 20: The results for the second case

Finally, in Figure 21 the correlation of inputs and outputs for both the model and the neural network prediction, for case 2 is depicted. One can observe that the neural network achieves better fitting in this case.

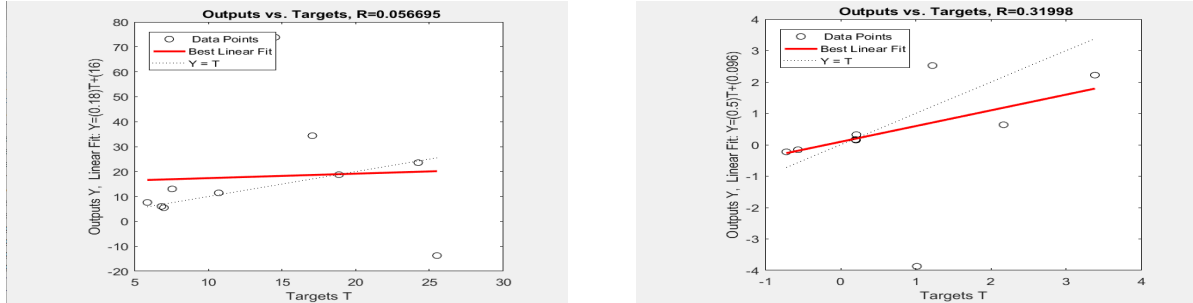


Figure 21: Correlation of inputs and outputs for both the model and the neural network prediction for case 2

8 Conclusion

In the present investigation two different cases were examined. The difference lies on the number and the position of the control points. From the results, one can conclude that a suitably trained neural network can predict effectively the positions of the recurring cracks, however only when the control points are evenly distributed along the surface of the wind turbine blade (case 2). It is also worth noting that only static loadings, and a relatively small amount of measurements were considered. A next step on the present investigation can be the optimization of the neural network characteristics, as well as the consideration of multiple loading which will be applied across every dimension. Moreover, an extension of this work to dynamic loadings with more measurements and the use of modal analysis tools can be also performed.

9 References

- Bouزيد O., Tian G.Y., Cumanan K. and Moore D., 2015, Structural Health Monitoring of Wind Turbine Blades: Acoustic Source Localization Using Wireless Sensor Networks, *Journal of Sensors*, vol. 2015, Article ID 139695, 11 pages, doi:10.1155/2015/139695.
- Efstathiades Ch., Baniotopoulos C., Nazarko P., Ziemianski L. and Stavroulakis G.E., 2007, Application of neural networks for the structural health monitoring in curtain-wall systems. *Engineering Structures*, 29, 3475-3484.
- Ghoshal A., Sundaresan M., Schulz M. and Pai P., 2000, Structural health monitoring techniques for wind turbine blades, *Journal of Wind Engineering and Industrial Aerodynamics*, 85(3), 309-324.
- Li H., Zhou W. and Xu J., 2014, Structural Health Monitoring of Wind Turbine Blades, in: *Wind Turbine Control and Monitoring* Eds. N. Luo, Y. Vidal, L. Acho, Springer, 231-265.
- Jensen M., 2008, Ultimate strength of a large wind turbine blade, Risø National Laboratory for Sustainable Energy and Department of Civil Engineering, Technical University of Denmark.
- Muradova A., Tairidis G. and Stavroulakis G., 2016 Adaptive Neuro-Fuzzy Vibration Control of a Smart Plate, *Numerical Algebra, Control and Optimization*, 7(3), 251-271, 2016
- Natke H., 1991, *Einführung in Theorie und Praxis der Zeitreihen- und Modalanalyse.*, Vieweg Verlag, 3rd edition, Braunschweig, Wiesbaden
- Protopapadakis E., Schauer M., Pierri E., Doulamis A., Stavroulakis G., Böhrnsen J. and Langer S., 2016, A genetically optimized neural classifier applied to numerical pile integrity tests considering concrete piles. *Computers and Structures*, 162, 68-79.
- Psychas I., Schauer M., Boehrnsen J-U., Marinaki M., Marinakis Y., Langer S. and Stavroulakis G., 2016, Detection of defective pile geometries using a coupled FEM/ SBFEM approach and an ant colony classification algorithm, *Acta Mechanica*, 227(5), 1279-1291.
- Rentoumis M., Koutsianitis P., Athanailidis I., Taridis G., Tselikos G., Bilalis N. and Stavroulakis G., 2018, Design and structural analysis of wind turbine blades for structural health monitoring consideration, 9th GRACM International Congress on Computational Mechanics, p.p. 153-162
- Stavroulakis G., 2013 *Inverse and crack identification problems in engineering mechanics.* Kluwer, 2000, reprinted by Springer. Stavroulakis G. and Antes H., 1997, Nondestructive elastostatic identification of unilateral cracks through BEM and Neural Networks, *Comput. Mech.* 20(5), 439-45

Stavroulakis G. and Antes H., 1998a, Crack detection in elastostatics and elastodynamics. A BEM modelling - neural network approach. In: Inverse Problems in Engineering Mechanics, Eds. M. Tanaka and G.S. Dulikravich, Proc. Intern. Symp. on Inverse Problems in Engineering Mechanics ISIP'98, Nagano City, Japan, March 24-27, Elsevier Science Ltd., pp. 81-90

Stavroulakis G. and Antes H., 1998b, Neural crack identification in steady state elastodynamics. *Computer Methods in Applied Mechanics and Engineering*, 165, 129-146.

Stavroulakis G. and Antes H., 1999a, Crack detection by elastostatic measurements. A neural network approach based on BEM modelling. In: Proceed. of IUTAM Symposium on Discretisation Methods in Structural Mechanics II, H.A. Mang, F.G. Rammerstorfer (eds), Vienna, 2-6 June 1997, Kluwer Academic Publishers, pp. 199-206.

Stavroulakis G. and Antes H., 1999b, Neural crack identification for quality control tasks. EFDAN'99 Fourth European Workshop on Fuzzy Decision Analysis and Recognition Technology, June 14-15, 1999, Dortmund, Germany, (ed.) R. Felix., Fuzzy Logik Systeme GmbH, 90-100.

Stavroulakis G., Engelhardt M., Likas A., Gallego R. and Antes H., 2004, Neural network assisted crack and flaw identification in transient dynamics. *Journal of Theoretical and Applied Mechanics*, Polish Academy of Sciences, Invited Paper in Special Issue on 'Engineering Applications of Soft Computing' 42(3), 629-649.

Tangier J. and Somers D., 1995, NREL Airfoil Families for HAWTs, NRELFTP-442-7109.

Kakoulli, E.; Soteriou, V.; Theocharides, T., "Intelligent Hotspot Prediction for Network-on-Chip-Based Multicore Systems," in *Computer-Aided Design of Integrated Circuits and Systems*, IEEE Transactions on , vol.31, no.3, pp.418-431, March 2012.

Lawrence S., Giles C.L., Tsoi A.C.: "Lessons in Neural Network Training: Overfitting May be Harder than Expected", *Proceedings of the Fourteenth National Conference on Artificial Intelligence*, AAAI-97, AAAI Press, Menlo Park, California, pp. 540-545, 1997.

Farrar, C. and K. Worden (2007). "An Introduction to Structural Health Monitoring." *The Philosophical Transactions of the Royal Society A*(365): pp. 303-315.

McGowan, J. G. (2000). *Windpower: A Turn of the Century Review*. *Annual Review of Energy and the Environment* , 25, 147-197.

RenewableUK 2012, "Wind farms hit high of more than 12% of UK electricity demand", [http://www.bwea.com/media/news/articles pr20120106.html](http://www.bwea.com/media/news/articles/pr20120106.html). Accessed on August 1, 2012.

Schreck.S.J & Robinson.M.C. 2007, "Horizontal axis wind turbine blade aerodynamics in experiments and modelling", IEEE transactions on energy conversion,vol. 22, no. 1.

REpower 2012, "Successful technological transfer: the REpower 5M offshore wind power plant", <http://www.repower.de/wind-power-solutions/wind-turbines/5m>. Accessed on August 1, 2012.

Quarton, D.C. The Evolution of Wind Turbine Design Analysis -A Twenty Year Progress Review; Garrad Hassan and Partners Ltd.: Bristol, UK, 1998; pp. 5–24.

Habali, S.M.; Saleh, I.A. Local design, testing and manufacturing of small mixed airfoil wind turbine blades of glass fiber reinforced plastics Part I: Design of the blade and root. Energy Convers. Manag. 2000, 41, 249–280.

Gasch, R.; Twele, J. Wind Power Plants; Solarpraxis: Berlin, Germany, 2002.

Burton, T. Wind Energy Handbook; John Wiley and Sons Ltd.: Chichester, UK, 2011.

Ahlstrom, A. Emergency stop simulation using a finite element model developed for large blade deflections. Wind Energy 2006, 9, 193–210.

Kong, C.; Bang, J.; Sugiyama, Y. Structural investigation of composite wind turbine blade considering various load cases and fatigue life. Energy 2005, 30, 2101–2114.

Brondsted, P.; Lilholt, H.; Lystrup, A. Composite materials for wind power turbine blades. Ann. Rev. Mater. Res. 2005, 35, 505–538. Jensen, F.M. Structural testing and numerical simulation of a 34-m composite wind turbine blade. Compos. Struct. 2006, 76, 52–61.

Veritas, D.N. Design and Manufacture of Wind Turbine Blades, Offshore and Onshore Turbines; Standard DNV-DS-J102; Det Norske Veritas: Copenhagen, Denmark, 2010.

Shokrieh, M.M.; Rafiee, R. Simulation of fatigue failure in a full composite wind turbine blade. Compos. Struct. 2006, 74, 332–342. Wind Turbines. Part 1: Design Requirements; BS EN 61400-1:2005; BSi British Standards: London, UK, January 2006.

Mølholt Jensen, Ultimate strength of a large wind turbine blade, Risø National Laboratory for Sustainable Energy & Department of Civil Engineering, Technical University of Denmark, 2008.

National Research Council, committee on Assessment of research needs for wind turbine rotor materials technology, Energy Engineering Board, Commission on Engineering and Technical Systems, Washington, ISBN: 0-309-58318-7, D.C. 1991.